Available online at www.sciencedirect.com
ScienceDirect
Trans. Nonferrous Met. Soc. China 30(2020) 463−471
Transactions of Nonferrous Metals Society of China
www.tnmsc.cn

Effects of SiC interfacial coating on mechanical properties of carbon fiber needled felt reinforced sol-derived Al_2O_3 composites

Kuan-hong ZENG, Qing-song MA, Xing-yu GU

Science and Technology on Advanced Ceramic Fibers & Composites Laboratory,
National University of Defense Technology, Changsha 410073, China

Received 2 July 2019; accepted 5 December 2019

Abstract: 3D carbon fiber needled felt and polycarbosilane-derived SiC coating were selected as reinforcement and interfacial coating, respectively, and the sol−impregnation−drying−heating (SIDH) route was used to fabricate C/Al_2O_3 composites. The effects of SiC interfacial coating on the mechanical properties, oxidation resistance and thermal shock resistance of C/Al_2O_3 composites were investigated. It is found that the fracture toughness of C/Al_2O_3 composites was remarkably superior to that of monolithic Al_2O_3 ceramics. The introduction of SiC interfacial coating obviously improved the strengths of C/Al_2O_3 composites although the fracture work diminished to some extent. Owing to the tight bonding between SiC coating and carbon fiber, the $C/SiC/Al_2O_3$ composites showed much better oxidation and thermal shock resistance over C/Al_2O_3 composites under static air.

Key words: alumina; carbon fiber reinforcement; interfacial coating; mechanical properties; oxidation resistance; thermal shock resistance

1 Introduction

Owing to high hardness, high strength and excellent thermal and chemical stabilities, alumina (Al_2O_3) ceramic is a desirable candidate for friction and wear applications under high velocity and heavy load conditions [1,2]. Unfortunately, the brittle fracture behavior of monolithic Al_2O_3 ceramic is disadvantageous to the friction and wear properties. Therefore, it is necessary to enhance the fracture toughness of monolithic Al_2O_3 ceramic.

Continuous fibers have been considered as the best reinforcement for toughening monolithic ceramics. So far, much attention on oxide fiber reinforced Al_2O_3 composites have been paid to [3−6]. On the contrary, the reports concerning SiC fiber or C fiber reinforced Al_2O_3 composites were rarely found [7,8]. In the study of COLOMBAN and WEY [8], three-dimensional (3D) carbon fiber needled felt reinforced Al_2O_3 (C/Al_2O_3) composites were fabricated through slurry infiltration and heat treatment, followed by alkoxide solution infiltration and pyrolysis for further densification. However, the flexural strength was low (~120 MPa). Furthermore, this technique is not suitable to manufacture large-size components with complex shape because of the sedimentation of slurry.

For the densification of 3D fiber preforms like the 3D fiber needled felt, vapor infiltration and liquid impregnation are preferable in order to achieve uniform distribution of matrix. If liquid impregnation is adopted, the choice of starting materials is important. The route from inorganic salt or alkoxide solution via sol−gel to Al_2O_3 ceramics has very low fabrication efficiency. Recently, the sol−impregnation−drying−heating (SIDH) route using the sol with high solid content as raw material has been employed to fabricate 3D fiber preform reinforced oxide ceramic composites [9−15]. Owing

Corresponding author: Qing-song MA; Tel: +86-731-87007601; Fax: +86-731-84576578; E-mail: nudtmqs1975@163.com
DOI: 10.1016/S1003-6326(20)65226-8

to the high solid content and the nano-sized colloidal particle, the SIDH route can improve fabrication efficiency of the route from solution via sol−gel to oxide ceramics and retain its advantages of low processing temperature and homogeneous distribution of oxide matrix.

In previous studies, we fabricated 3D carbon fiber preforms reinforced mullite [12,16], YAG (yttrium aluminum garnet, $Y_3Al_5O_{12}$) [14,15] through the SIDH route. In addition, the Al_2O_3 composites reinforced with the laminated and stitched carbon fiber cloth were also prepared by the SIDH route [13]. It was indicated that the characteristics of sol and the structure of fiber preform had great influence on the processing and mechanical properties of 3D fiber composites. Therefore, the processing of SIDH route should not be simply copied for different 3D fiber preform reinforced oxide composites.

In addition to densification technologies, interface is very important for fiber reinforced ceramic matrix composites. For oxide fibers/Al_2O_3 composites, several kinds of interfacial coatings have been developed to avoid the formation of chemically bonded interface [3−6,9,10]. For SiC/Al_2O_3 composites, BN/SiC double-layer interfacial coating was prepared by chemical vapor deposition to protect SiC fiber from the oxidation [7] because the Al_2O_3 matrix was obtained by the oxidation of liquid Al. However, the effects of interfacial coating on the performance of C/Al_2O_3 composites were less investigated.

Aiming at the friction and wear applications and from the experience of C/C, C/SiC or C/C−SiC brakes [17−19], 3D carbon fiber needled felt reinforced Al_2O_3 composites with SiC coating as interphase were fabricated through the SIDH route in this work. The processing and the effect of interfacial coating on mechanical properties of C/Al_2O_3 composites under various environments were discussed.

2 Experimental

2.1 Materials and processing

The Al_2O_3 sol used in this study was the same as that in previous work [13]. The solid content, pH, colloid particle diameter and viscosity of Al_2O_3 sol were 30 wt.%, 2.7, 20−30 nm and 12−13 mPa·s, respectively. The thermal analysis, phase evolution and sintering shrinkage of the Al_2O_3 gel powder were studied in our previous work [13]. The 3D carbon fiber needled felt consisted of T300 carbon fiber plain cloth and T700 short-cut carbon fiber web. One unit-layer was composed of a ply of 0° plain cloth and a ply of short-cut fiber web, stacked with 90° plain cloth ply and then another short-cut fiber web ply. After the desired thickness was reached, needling process was performed to keep adjacent units together with carbon fibers carried. The obtained 3D carbon fiber needled felt had a fiber volume fraction of 24%.

Prior to the preparation of C/Al_2O_3 composites, the 3D carbon fiber needled felt was de-sized at 1400 °C [20]. Then, the felt was impregnated with the Al_2O_3 sol under vacuum. After being soaked in the sol for 4 h, the felt was dried at 200 °C for 4 h in air, followed by heat treatment at 1100 °C for 1 h under the protection of high purity Ar. The cycle of impregnation−drying−heat treatment was repeated 33 times to obtain C/Al_2O_3 composites. To study the effect of interfacial coating on properties of C/Al_2O_3 composites, SiC coating was prepared on the surface of carbon fibers after de-sizing. Considering the homogeneousness and reliability of coating, especially in case of large-size component with complex shape, polycarbosilane (PCS) pyrolysis was employed to prepare SiC coating. The de-sized carbon fiber needled felt was impregnated with PCS/xylene solution under vacuum. The mass fraction of PCS in solution was 5%. After being soaked in PCS/xylene solution for 4 h, the felt was taken out and dried at 80 °C for 4 h in air, followed by pyrolysis at 1600 °C for 1 h under the protection of high purity Ar. The cycle of PCS solution impregnation and pyrolysis was repeated 3 times to obtain SiC coating. Then, the Al_2O_3 matrix was introduced by the above-mentioned SIDH procedure. The obtained composites were named C/SiC/Al_2O_3 composites.

The as-fabricated C/Al_2O_3 and C/SiC/Al_2O_3 composites were oxidized and thermally shocked under static air. The oxidation was carried out at 400, 600, 800 and 1000 °C for 30 min, respectively. The thermal shock was performed from 400, 600, 800 and 1000 °C to room temperature, respectively.

The muffle was heated to preset temperature. Then, the sample was put into muffle. After being soaked for 10 min, the sample was moved out of muffle. After being cooled to room temperature, the sample was put into muffle again. The thermal shock was repeated 10 times.

2.2 Characterization methods

According to the density mixing law, the theoretic density (ρ_T) of C/Al_2O_3 composites was calculated from the equation of $\rho_T=V_f \cdot \rho_f+V_m \cdot \rho_m$, where V_f and V_m are the volume fractions of fiber (24%) and matrix (76%), and ρ_f and ρ_m are the true densities of fiber (1.76 g/cm^3) and Al_2O_3 matrix (3.90 g/cm^3), respectively. The apparent density (ρ_a) was obtained from the mass-to-volume ratio. Thus, total porosity was equal to $1-(\rho_a/\rho_T)$.

The as-fabricated composites were cut into the samples with a size of 70 mm (length) × 5 mm (width) × 4 mm (height) for the flexural strength test. The flexural strength was measured by three-point bending test with a cross-head speed of 0.5 mm/min and a span-to-height ratio of 15:1. Fracture work was calculated from the formula of $W=A_C/(B \cdot H)$ [21], where A_C is the characteristic area of fracture curve, which refers to the area under load–displacement curve above 90% stress; H and B are the thickness and width of the sample, respectively. The samples for interlaminar shear strength test had the size of 30 mm (length) × 5 mm (width) × 4 mm (height). Short beam method was employed to measure interlaminar shear strength with a cross-head speed of 0.5 mm/min and a span-to-height ratio of 5:1. The samples with a size of 12 mm × 4 mm × 4 mm were cut from the as-prepared composites for the compressive strength test. The compressive strength test was carried out on Z direction of sample. The Z direction was perpendicular to carbon fiber cloth. The composites were machined into dog-bone shaped samples for tensile strength test. Five specimens were tested to obtain average strength.

Mass loss and flexural strength retention after oxidation and thermal shock were recorded to characterize the oxidation resistance and thermal shock resistance of the composites. Scanning electron microscopy (SEM, Quanta FEG 250) was employed to observe the microstructure of the composites.

3 Results and discussion

3.1 Effects of SiC interfacial coating on mechanical properties of C/Al_2O_3 composites

The apparent density of C/Al_2O_3 composites was measured to be 2.68 g/cm^3 from the mass-to-volume ratio. According to the density mixing law, the theoretical density was computed to be 3.39 g/cm^3. Thus, the total porosity is calculated to be 20.8%. Figure 1 shows the cross-sections of C/Al_2O_3 composites and Al_2O_3 matrix. As shown in Fig. 1(a), carbon fiber preform was well filled by

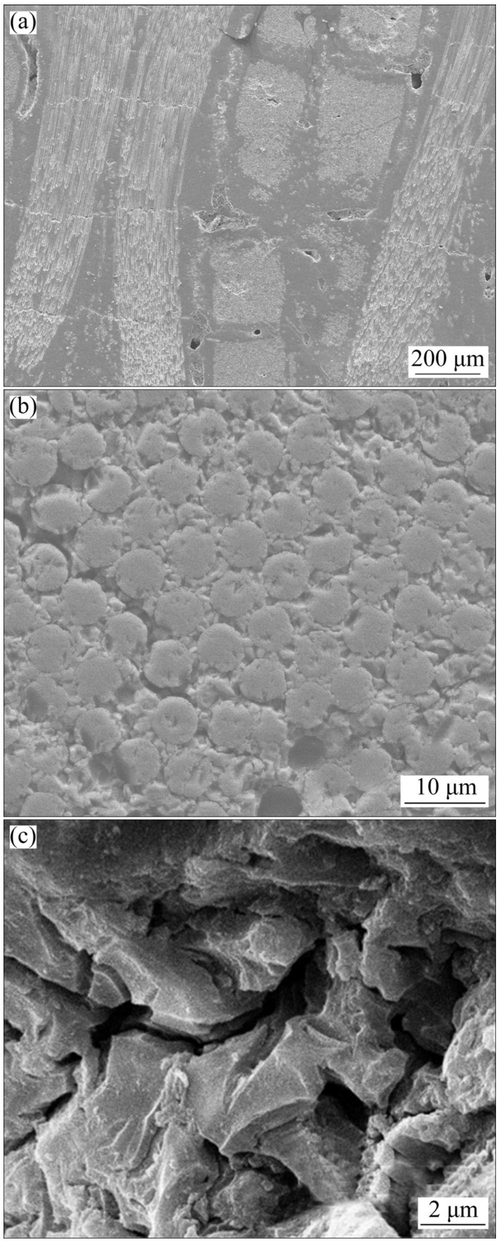

Fig. 1 Cross-sectional morphologies of C/Al_2O_3 composites (a, b) and Al_2O_3 matrix (c)

Al_2O_3 matrix, and the cross-section was relatively dense except several large pores. Due to the low viscosity and the nano-sized colloid particles, it is easy for Al_2O_3 sol to diffuse into carbon fiber needled felt in early cycles. With the increase of density, the diffusion channels became narrow and wandering. Thus, some voids were not occupied by Al_2O_3 matrix. When the diffusion channels were completely clogged, the closed pores formed. Besides the large closed pores, as shown in Figs. 1(b) and (c), the composites contained some small pores and some microcracks. The microcracks resulted from the under-sintering of Al_2O_3 matrix at 1100 °C and the thermal mismatch between carbon fiber and Al_2O_3 matrix. The small pores inside fiber bundle could also be attributed to the diffusion of sol.

In comparison with the carbon fiber needled felt reinforced YAG (C/YAG) composites [15] which were also fabricated by SIDH route, the vertical cracks in fiber web and the gaps between fiber cloth and fiber web were not observed in this study. This phenomenon is related with the state of thermal stress. On one hand, the discrepancy of thermal expansion coefficients between carbon fiber and Al_2O_3 is less than that between carbon fiber and YAG. On the other hand, the heat treatment was carried out at 1100 °C in this study whereas the highest temperature of heat treatment was 1600 °C for the fabrication of C/YAG composites. At 1100 °C, the Al_2O_3 matrix exhibited a sintering linear shrinkage of ~13% [13]. The linear shrinkage of YAG at 1600 °C was ~23% [14]. Due to the smaller thermal mismatch between carbon fiber and Al_2O_3 matrix and the lower linear shrinkage, the thermal stress in C/Al_2O_3 composites was lower than that in C/YAG composites.

Table 1 lists the mechanical properties of C/Al_2O_3 and $C/SiC/Al_2O_3$ composites. The flexural strength, fracture work and compressive strength of C/Al_2O_3 composites were 155.9 MPa, 6772.2 J/m^2 and 274.2 MPa, respectively, which could meet the demands of brake application. Moreover, considering the high total porosity of 20.8%, the mechanical properties of C/Al_2O_3 composites are favorable. Figures 2 and 3 show the fracture surface and the stress−strain curve of C/Al_2O_3 composites, respectively. Extensive fiber pull-out and long pull-out length were observed clearly. The flexural strain was as high as 2.5%. These results indicated that the C/Al_2O_3 composites exhibited non-catastrophic fracture behavior and the fracture toughness of monolithic Al_2O_3 ceramics was enhanced notably.

Table 1 Mechanical properties of C/Al_2O_3 and $C/SiC/Al_2O_3$ composites

Property	C/Al_2O_3 composite	$C/SiC/Al_2O_3$ composite
Apparent density/(g·cm^{-3})	2.68	2.91
Total porosity/%	20.8	14.2
Flexural strength/MPa	155.9	168.1
Fracture work/(J·m^{-2})	6772.2	4828.3
Interlaminar shear strength/MPa	10.9	21.2
Compressive strength/MPa	274.2	468.8
Tensile strength/MPa	63.4	90.2

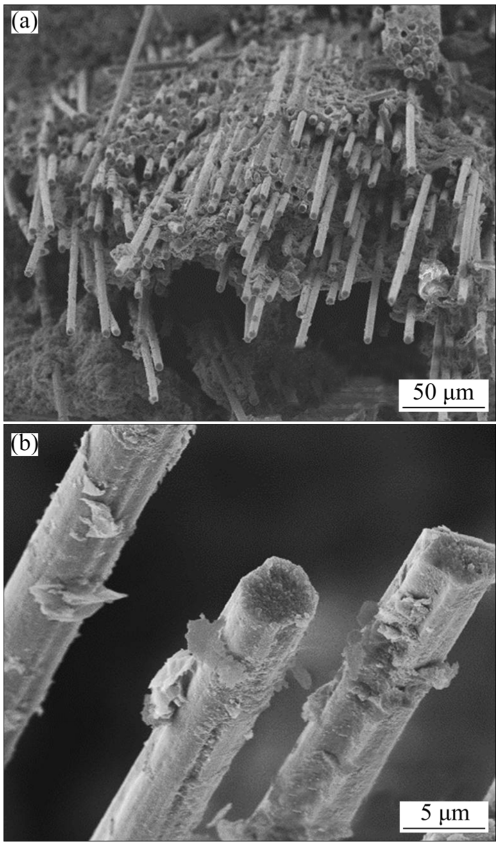

Fig. 2 Morphologies of fracture surfaces for C/Al_2O_3 composites

Fiber reinforced ceramic matrix composites are often fabricated at high temperature. Sometimes, high pressure is also required. Therefore, it is very likely to form strong interfacial bonding. Once the

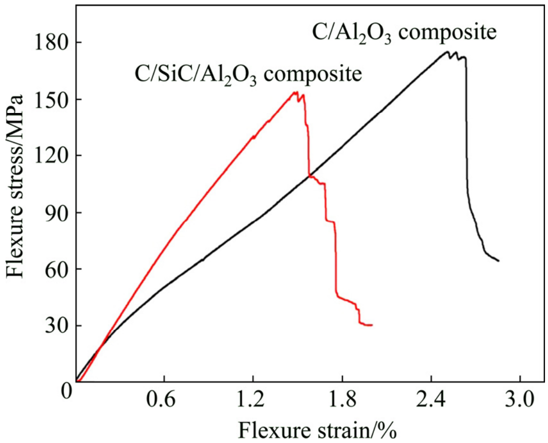

Fig. 3 Stress−strain curves of C/Al_2O_3 and $C/SiC/Al_2O_3$ composites

strong interfacial bonding belongs to the chemical bonding, the mechanical properties of composites are affirmatively low because fibers are destroyed by chemical reaction. In this study, the heat treatment during fabrication of C/Al_2O_3 composites was performed at 1100 °C without pressure. In this case, the formation of strong chemical bonding was impossible. As mentioned above, the Al_2O_3 matrix was porous and under-sintered. The thermal stress derived from the mismatch of thermal expansion between carbon fiber and Al_2O_3 matrix could be released. Thus, strong physical bonding was also difficult to create. As a result, C/Al_2O_3 composites showed high fracture work and flexural strain. In our previous study [13], the laminated and stitched carbon fiber cloth reinforced Al_2O_3 composites were fabricated at 1400 °C and had a total porosity of 15.5%. Due to the higher processing temperature and lower total porosity, the interfacial bonding was relatively strong, resulting in lower flexural strain and fracture work (3259.6 J/m^2).

The morphology of SiC coating is shown in Fig. 4. It is shown that carbon fiber was well coated by SiC. The SiC coating was dense and smooth, and its thickness was about 250 nm. The microstructure of $C/SiC/Al_2O_3$ composites is displayed in Fig. 5. In comparison with C/Al_2O_3 composites (Fig. 1), the quantity and size of pores in $C/SiC/Al_2O_3$ composites obviously decreased. Thus, it is found from Table 1 that the $C/SiC/Al_2O_3$ composites had lower total porosity. By comparing Fig. 5(b) with Fig. 1(b), it is evident that the intra-bundle density of $C/SiC/Al_2O_3$ composites was higher than that of C/Al_2O_3 composites. As compared with the water-

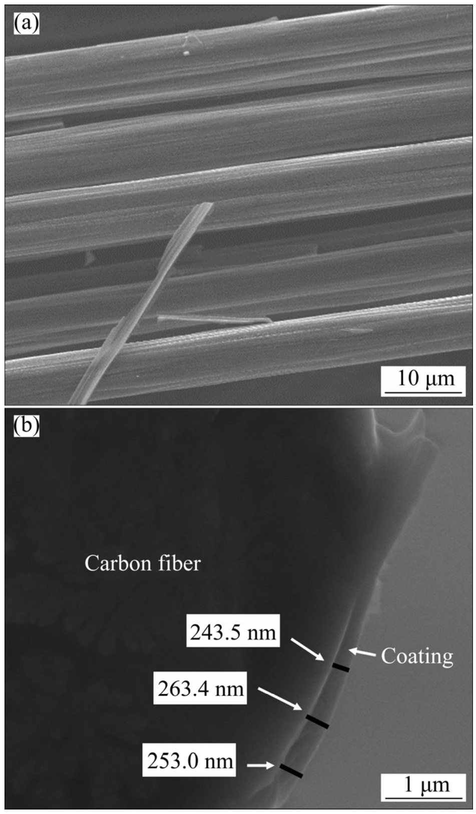

Fig. 4 SEM images of surface (a) and cross-section (b) of SiC-coated carbon fiber

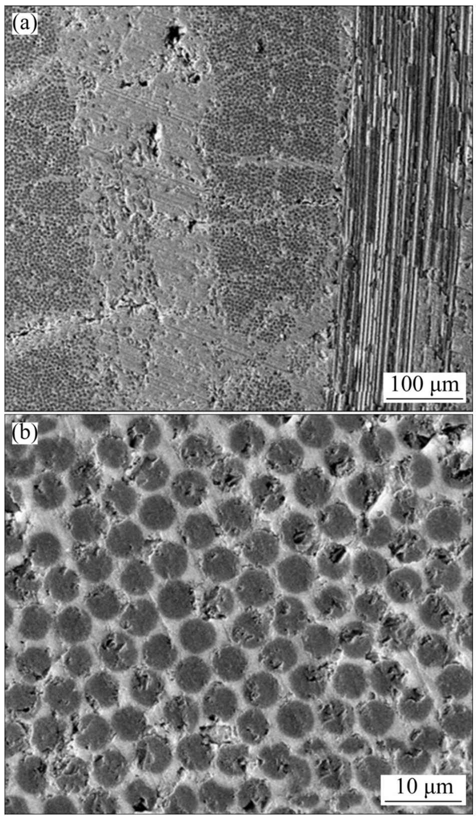

Fig. 5 SEM images of cross-section of $C/SiC/Al_2O_3$ composites

based Al_2O_3 sol, it is easier for the PCS/xylene solution to diffuse into intra-bundle space. In addition, SiC coating has a thermal expansion coefficient between that of carbon fiber and Al_2O_3. As a result, the interfacial microcracks were reduced.

Due to the good affinity between PCS and carbon fiber and the relatively smaller thermal expansion discrepancy between SiC and carbon fiber, stronger interfacial bonding was created for C/SiC/Al_2O_3 composites. In Fig. 6, fiber pull-out was not as extensive as that of C/Al_2O_3 composites. And the surface of pull-out fibers was smoother, which was due to the debonding from the SiC/Al_2O_3 interface. Accordingly, as listed in Table 1, the fracture work of C/SiC/Al_2O_3 composites was lower than that of C/Al_2O_3 composites. At the same time, it is found from Fig. 3 that the flexural strain of C/SiC/Al_2O_3 composites was about 1.5%, which was less than that of C/Al_2O_3 composites. However, the strong interfacial bonding still belonged to physical bonding. In this situation, the fiber strength was not obviously impaired. Moreover, the strong interfacial bonding is beneficial to the load-transfer from matrix to carbon fibers. Consequently, the flexural strength, interlaminar shear strength, compressive strength and tensile strength were promoted owing to the high strength of carbon fibers. Especially, the interlaminar shear strength, compressive strength and tensile strength were increased to a great extent.

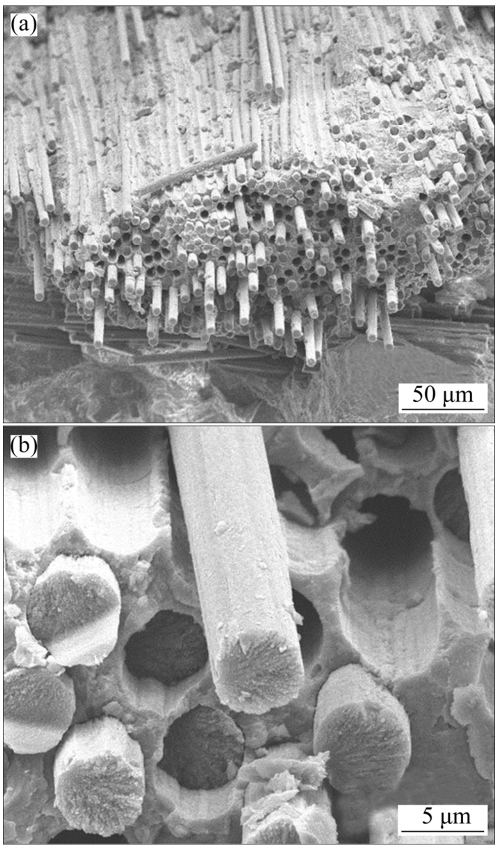

Fig. 6 Morphologies of fracture surfaces for C/SiC/Al_2O_3 composites

3.2 Effects of SiC interfacial coating on oxidation and thermal shock resistance of C/Al_2O_3 composites

The mass loss and flexural strength retention ratio of C/Al_2O_3 and C/SiC/Al_2O_3 composites after oxidation and thermal shock are presented in Tables 2 and 3, respectively. For the C/Al_2O_3 composites, mass loss and flexural strength loss were detected from 400 °C because of their porous microstructure (Fig. 1). With the elevation of temperature, mass loss and flexural strength loss increased. Since the Al_2O_3 matrix is immune to oxidation, the mass loss can be ascribed to the oxidation of carbon fibers. As shown in Fig. 7(a), the interface gaps resulting from the oxidation of carbon fibers were visible. After

Table 2 Oxidation resistance of C/Al_2O_3 and C/SiC/Al_2O_3 composites

Oxidation temperature/°C	C/Al_2O_3 composite		C/SiC/Al_2O_3 composite	
	Mass loss/%	Flexural strength retention ratio/%	Mass loss/%	Flexural strength retention ratio/%
400	0.2	95.3	−	−
600	1.1	45.2	−	−
800	1.9	51.2	1.0	99.7
1000	2.4	57.7	2.0	100

Table 3 Thermal shock resistance of C/Al_2O_3 and C/SiC/Al_2O_3 composites

Thermal shock temperature/°C	C/Al_2O_3 composite		C/SiC/Al_2O_3 composite	
	Mass loss/%	Flexural strength retention ratio/%	Mass loss/%	Flexural strength retention ratio/%
400	0.4	66.7	—	—
600	3.4	18.2	—	—
800	5.0	21.7	2.6	97.4
1000	5.8	28.3	3.8	83.1

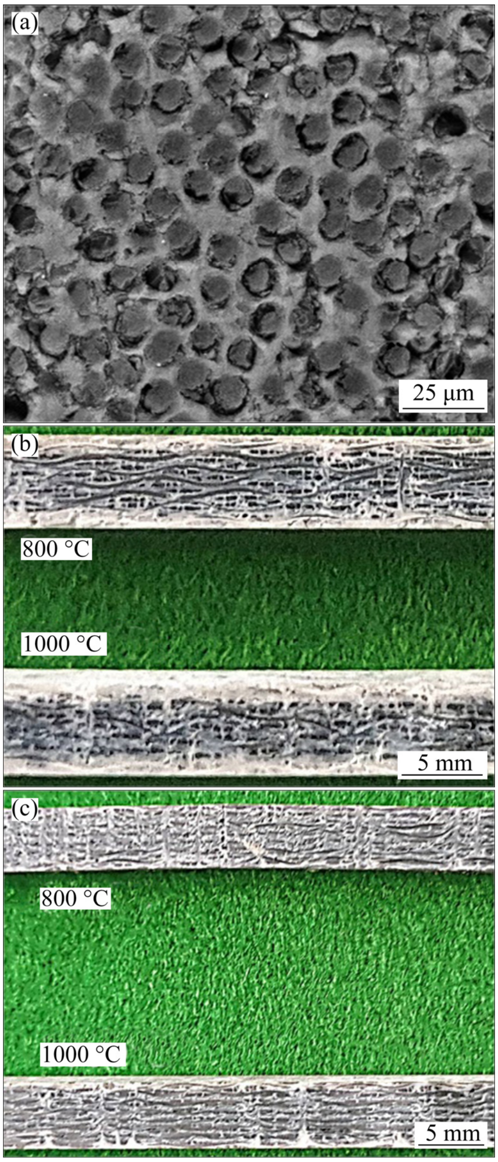

Fig. 7 SEM image of cross-section of C/Al_2O_3 composites after oxidation at 1000 °C (a) and optical images of side faces of C/Al_2O_3 (b) and $C/SiC/Al_2O_3$ (c) composites after oxidation

oxidation, the sample was cut. Figure 7(b) shows the optical image of the side face. The surface of sample was white and the interior was black, indicating that the oxidation occurred from surface to interior. In addition, the white layer thickened from 800 to 1000 °C, implying that the oxidation depth increased with the elevation of temperature.

It is noticed that the mass loss and flexural strength loss after thermal shock were much higher than those after oxidation. Firstly, 10 times of thermal shock in air corresponded to static oxidation for 100 min, whereas the static oxidation was carried out only for 30 min. Secondly, the thermal stress was enlarged during thermal shock, creating more diffusion channels for oxygen and impairing the load-bearing capacity of matrix. By comparing Figs. 7(a, b) with Figs. 8(a, b), the severer oxidation of carbon fibers during thermal shock was very apparent.

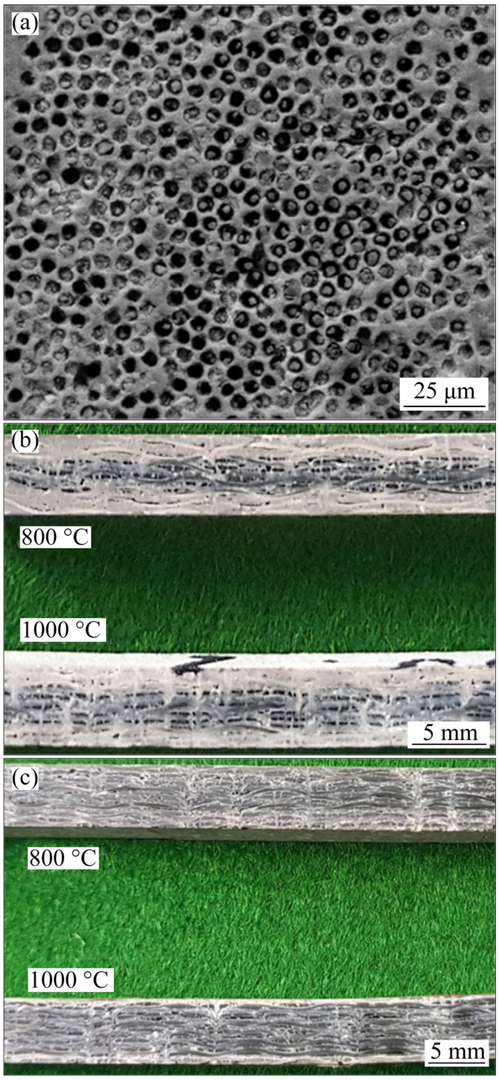

Fig. 8 SEM image of cross-section of C/Al_2O_3 composites after thermal shock at 1000 °C (a) and optical images of side faces of C/Al_2O_3 (b) and $C/SiC/Al_2O_3$ (c) composites after thermal shock

In addition, it seems strange that the flexural strength retention ratio was increased with the elevation of temperature from 600 to 1000 °C, whereas the mass loss was on the contrary. In our previous studies [15,22], this phenomenon was considered to be related with the state of microcracks during static oxidation and thermal shock. The C/Al_2O_3 composites were fabricated at 1100 °C and had some microcracks when the composites were cooled to room temperature due to the thermal mismatch between carbon fiber and Al_2O_3 matrix. When static oxidation and thermal shock were performed at 1000 °C, these microcracks could be better healed. The closure of microcracks could enhance the load-bearing capacity of matrix to a certain extent, which was responsible for the higher flexural strength retention ratio at 1000 °C. Of course, the microcracks could not be entirely closed. With the elevation of temperature, the oxidation of carbon fibers became serious. Therefore, the mass loss still increased from 600 to 1000 °C.

By comparison, the positive effects of SiC interfacial coating on the oxidation and thermal shock resistance of C/Al_2O_3 composites are significant. After static oxidation at 800 and 1000 °C, no flexural strength degradation was observed for the $C/SiC/Al_2O_3$ composites. After thermal shock at 800 and 1000 °C, the flexural strength ratios were above 80%. In Figs. 7 and 8, it is clear that the oxidation degrees of $C/SiC/Al_2O_3$ composites were much lower than those of C/Al_2O_3 composites. As mentioned above, SiC coating was tightly bonded to carbon fibers. Thus, carbon fibers can be effectively protected by the viscous SiO_2 derived from the oxidation of SiC coating during static oxidation and thermal shock. However, there is thermal mismatch between carbon fiber and SiC coating. Microcracks were probable to form at fiber/coating interface during thermal shock, leading to larger mass loss than that during static oxidation. With regard to the mass loss under static oxidation, it may be caused by the attack of oxygen from the end of carbon fiber. This oxidation mode exhibited the characteristics of large range and low degree. Namely, many carbon fibers were oxidized to a very low degree. As a result, the flexural strength almost did not decrease.

4 Conclusions

(1) 3D carbon fiber needled felt reinforced Al_2O_3 composites have been fabricated through the SIDH route using the Al_2O_3 sol with a high solid content as raw materials. Thanks to the reinforcement of 3D carbon fiber needled felt, the fracture work of C/Al_2O_3 composites was as high as 6772.2 J/m^2 which was much higher than that of monolithic Al_2O_3 ceramics. Although the total porosity reached 20.8%, the C/Al_2O_3 composites showed favorable strengths.

(2) The fracture work decreased to 4828.3 J/m^2 by introducing polycarbosilane-derived SiC interfacial coating, but the flexural strength, interlaminar shear strength, compressive strength and tensile strength were increased to 168.1, 21.2, 468.8 and 90.2 MPa, by 94.5%, 71.0% and 42.3%, respectively.

(3) Due to the protection of SiC coating, the oxidation and thermal shock resistance of C/Al_2O_3 composites were enhanced notably. The flexural strength of $C/SiC/Al_2O_3$ composites kept unchanged after oxidation at 1000 °C for 30 min. After 10 times of thermal shock from 1000 °C to room temperature under static air, the $C/SiC/Al_2O_3$ composites retained 83.1% of original flexural strength. In all, $C/SiC/Al_2O_3$ composites are promising candidates for friction and wear applications.

References

[1] WU Ting-ting, ZHOU Jian, WU Bo-lin, XIONG Yuan. Effect of Y_2O_3 additives on the wet abrasion resistance of an alumina-based grinding medium [J]. Wear, 2016, 356−357: 9−16.

[2] YAZDANI A, ISFAHANI T. A facile method for fabrication of nano-structured Ni−Al_2O_3 graded coatings: Structural characterization [J]. Transactions of Nonferrous Metals Society of China, 2018, 28: 77−87.

[3] POGES S, MONTELEONE C, PETROSKI K, RICHARDS G, SUIB S L. Preparation and characterization of an oxide-oxide continuous fiber reinforced ceramic matrix composite with a zinc oxide interphase [J]. Ceramics International, 2017, 43: 17121−17127.

[4] CHEN Z C, TAMACHI T, KULKARNI R, CHAWLA K K, KOOPMAN M. Interfacial reaction behavior and thermal stability of barium zirconate-coated alumina fiber/alumina matrix composites [J]. Journal of the European Ceramic Society, 2018, 28: 1149−1160.

[5] LICCIULLI A, CHIECHI A, FERSINI M, SANOSH K P. Influence of zirconia interfacial coating on alumina fiber-reinforced alumina matrix composites [J]. International Journal of Applied Ceramic Technology, 2013, 10(2): 251−256.

[6] JACKSON P R, RUGGLES-WRENN M B, BAEK S S, KELLER K A. Compressive creep behavior of an oxide–oxide ceramic composite with monazite fiber coating at elevated temperatures [J]. Materials Science and Engineering A, 2007, 454−455: 590−601.

[7] WILSHIRE B, CARREÑO F. Deformation and damage processes during tensile creep of ceramic-fibre-reinforced ceramic-matrix composites [J]. Journal of the European Ceramic Society, 2000, 20: 463−472.

[8] COLOMBAN Ph, WEY M. Sol−gel control of matrix net-shape sintering in 3D fibre reinforced ceramic matrix composites [J]. Journal of the European Ceramic Society, 1997, 17: 1475−1483.
[9] WANG Yi, LIU Hai-tao, CHENG Hai-feng, WANG Jun. Effective fugitive carbon coatings for the strength improvement of 3D Nextel^{TM} 440/aluminosilicate composites [J]. Materials Letters, 2014, 126: 236−239.
[10] WANG Yi, CHENG Hai-feng, WANG Jun. Effects of the single layer CVD SiC interphases on mechanical properties of mullite fiber-reinforced mullite matrix composites fabricated via a sol−gel process [J]. Ceramics International, 2014, 40(3): 4707−4715.
[11] WANG Qing, CAO Feng, XIANG Yang, PENG Zhi-hang. Effects of ZrO_2 coating on the strength improvement of 2.5D SiC_f/SiO_2 composites [J]. Ceramics International, 2017, 43(1): 884−889.
[12] ZHANG Wei, MA Qing-song, DAI Ke-wei, MAO Wei-guo. Preparation of three-dimensional braided carbon fiber reinforced mullite composites from a sol with high solid content [J]. Transactions of Nonferrous Metals Society of China, 2018, 28: 2248−2254.
[13] FAN Chao-yang, MA Qing-song, ZENG Kuan-hong. Thermal stability and oxidation resistance of C/Al_2O_3 composites fabricated from a sol with high solid content [J]. Ceramics International, 2017, 43(14): 10983−10990.
[14] SHAN Bo-rong, MA Qing-song, ZENG Kuan-hong. Fabrication of three-dimensional carbon fiber preform reinforced YAG composites from a sol with high solid content [J]. Ceramics International, 2018, 44(4): 4478−4482.
[15] SHAN Bo-rong, MA Qing-song, ZENG Kuan-hong. Microstructure and mechanical properties of carbon fiber needled felt reinforced sol-derived YAG composite [J]. Journal of Alloys and Compounds, 2019, 772: 381−387.
[16] ZHANG Wei, MA Qing-song, ZENG Kuan-hong, LIANG Song-lin, MAO Wei-guo. Mechanical properties and thermal stability of carbon fiber cloth reinforced sol-derived mullite composites [J]. Journal of Advanced Ceramics, 2019, 8(2): 218−227.
[17] CHEN Guan-yi, LI Zhuan, XIAO Peng, OUYANG Xi, MA Wen-jie, LI Peng-tao, LI Jin-wei, LI Yang. Tribological properties and thermal-stress analysis of C/C−SiC composites during braking [J]. Transactions of Nonferrous Metals Society of China, 2019, 29: 123−131.
[18] GE Yi-cheng, YANG Ling-yun, WU Shuai, LI Chan, LUO Jian, YI Mao-zhong. Influence of heat-treatment on oxidation-resistance of phosphate-coating for C/C composite [J]. Transactions of Nonferrous Metals Society of China, 2014, 24: 455−461.
[19] ZHANG Jian-xin, FAN Shang-wu, ZHANG Li-tong, CHENG Lai-fei, YANG Shang-jie, TIAN Guang-lai. Microstructure and frictional properties of 3D needled C/SiC brake materials modified with graphite [J]. Transactions of Nonferrous Metals Society of China, 2010, 20: 2289−2293.
[20] LIU H T, YANG L W, SUN X, CHENG H F, WANG C Y, MAO W G, MOLINA-ALDAREGUIA J M. Enhancing the fracture resistance of carbon fiber reinforced SiC matrix composites by interface modification through a simple fiber heat-treatment process [J]. Carbon, 2016, 109: 435−443.
[21] LIU Yong-sheng, CHENG Lai-fei, ZHANG Li-tong, YANG Wen-bin, ZHOU Sheng-tian, ZHANG Wei-hua. Fracture behavior and mechanism of 2D C/SiC−BC_x composite at room temperature [J]. Materials Science and Engineering A, 2011, 528: 1436−1441.
[22] SHAN Bo-rong, MA Qing-song, ZENG Kuan-hong. Thermal shock resistance of carbon fiber preform reinforced sol-derived YAG composites [J]. Ceramics International, 2019, 45(5): 6560−6565.

SiC 界面涂层对碳纤维针刺毡增强 Al_2O_3 复合材料力学性能的影响

曾宽宏，马青松，顾星宇

国防科技大学 新型陶瓷纤维及其复合材料重点实验室，长沙 410073

摘　要：分别采用 3D 碳纤维针刺毡为增强体以及聚碳硅烷(PCS)衍生 SiC 涂层为界面相，通过溶胶−浸渍−干燥−热处理 (SIDH) 技术制备 C/Al_2O_3 复合材料，研究 SiC 界面涂层对 C/Al_2O_3 复合材料力学性能、抗氧化性能和抗热震性能的影响。结果表明，C/Al_2O_3 复合材料的断裂韧性显著优于 Al_2O_3 单体陶瓷，引入 SiC 界面涂层后，尽管断裂功有一定程度下降，但 C/Al_2O_3 复合材料的强度得到明显提高；得益于 SiC 涂层和 C 纤维之间的强结合，$C/SiC/Al_2O_3$ 复合材料在静态空气中表现出明显优于 C/Al_2O_3 复合材料的抗氧化和抗热震性能。

关键词：氧化铝；碳纤维增强体；界面涂层；力学性能；抗氧化性能；抗热震性能

(Edited by Bing YANG)